ADVANCED HEALTHCARE MATERIALS
www.advhealthmat.de

Conjugated Polymer for Implantable Electronics toward Clinical Application

*Yuxin Liu, Vivian Rachel Feig, and Zhenan Bao**

Owing to their excellent mechanical flexibility, mixed-conducting electrical property, and extraordinary chemical turnability, conjugated polymers have been demonstrated to be an ideal bioelectronic interface to deliver therapeutic effect in many different chronic diseases. This review article summarizes the latest advances in implantable electronics using conjugated polymers as electroactive materials and identifies remaining challenges and opportunities for developing electronic medicine. Examples of conjugated polymer-based bioelectronic devices are selectively reviewed in human clinical studies or animal studies with the potential for clinical adoption. The unique properties of conjugated polymers are highlighted and exemplified as potential solutions to address the specific challenges in electronic medicine.

1. Introduction

Electronic medicine is an emerging field that uses electricity to regulate and interact with biological tissues, especially electrogenic tissue, delivering high-temporospatial-resolution and personalized therapy. In the past two decades, the rapid development of organic bioelectronics and understanding of neurophysiology (e.g., inflammatory reflex) opens up many opportunities. Electronic medicine has been used to treat a variety of chronic diseases, such as atrial fibrillation, epilepsy and Parkinson's disease by sending or collecting electrical signals. In contrast to pharmaceutical medicine that modulates biochemical signaling in biological systems, electronic medicine transports charges across the interface between electronics and biological tissue to manage and treat diseases. Implantable electronic medicine has been used to treat millions of patients, with an expected annual market size of over 20 billion by 2022.[1] For drug-resistant diseases, such as drug-resistant epilepsy, electronic medicine serves as the last resort for alleviating the symptoms.

In current clinical practice, metal-based conductors, such as platinum and gold, remain the primary electronic materials to inject charges in and out of the biotic-abiotic interface. However, conjugated polymers, with their unique mechanical, chemical, and electrical properties, are becoming an attractive alternative for interfacing with biological tissue. Common conjugated polymers with biomedical potential include semiconducting polymer[2]–[9] such as poly(3-hexylthiophene) (P3HT)[10] and conducting polymer such as poly(3,4-ethylenedioxythiophene) polystyrene sulfonate (PEDOT:PSS),[11] polyaniline,[12] polypyrrole(Ppy)[13] (**Figure 1**).

In this review, we summarize the latest advances on using conjugated polymers for implantable electronics. We do not include on-skin wearable electronics, which have been extensively covered by other reviews.[14]–[16] We focus specifically on polymeric devices that have been shown feasibilities in human clinical studies or animal studies with potential for clinical adoption. In the clinical applications, conjugated polymers play a critical role for delivering charges to modulate electrogenic tissues, and for sensing the electrophysiological signals and controlling the release of biomolecular compounds at the interfaced tissues. The review is structured according to different biological and clinical applications that exemplify and highlight one or more unique properties of conducting polymers. In the following sections, we will first highlight some of the unique advantages of conjugated polymers in bioelectronics. The following sections are organized based on clinically-relevant and disease-associated physiological application including intracranial, peripheral nerve, cardiac, biomolecular, and emerging distributed interfaces. The review concludes with pointing out the remaining challenges and opportunities for developing clinically-translatable conjugated polymer-based tissue-mimicking implantable electronics.

2. Advantages of Conjugated Polymers in Bioelectronics

2.1. Mixed Conductor

Electrophysiological communication and function of biological tissues and cells is based on the mobility of the hydrated ions presented in intra- and extracellular environment. The mismatch

Dr. Y. Liu
Institute of Materials Research and Engineering
Agency for Science, Technology and Research
Singapore 138634, Singapore
Dr. V. R. Feig
Division of Gastroenterology, Department of Medicine, Brigham and Women's Hospital
Harvard Medical School
Boston, MA 02115, USA
Prof. Z. Bao
Department of Chemical Engineering
Stanford University
Stanford, CA 94305, USA
E-mail: zbao@stanford.edu

The ORCID identification number(s) for the author(s) of this article can be found under https://doi.org/10.1002/adhm.202001916

DOI: 10.1002/adhm.202001916

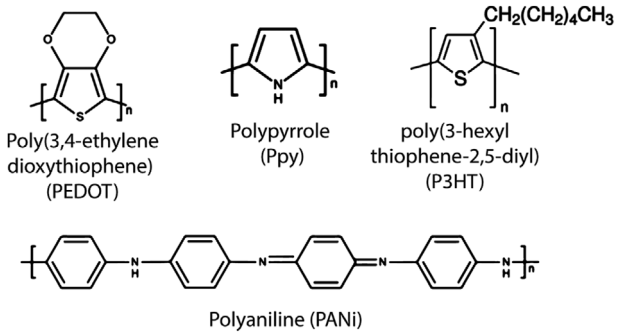

Figure 1. Chemical structures of common conductive polymers for bioelectronic applications: poly(3,4-ethylenedioxythiophene), polypyrrole, poly(3-hexylthiophene-2,5-diyl) and polyaniline.

of the ionic conduction in electrogenic tissues and electronic conduction in conventional inorganic materials pose a challenge for effective electrical therapeutics. Different from metal conductors, conjugated polymers form contiguous $SP^{[2]}$ -hybridized carbon centers with alternating double and single bonds in the backbone. The delocalized π-orbitals facilitate charge transport intra- and intermolecularly.[17] Doping is a common strategy to increase the conductivity of conjugated polymers by charge transfer to or from the doping molecules to the conjugated polymer to generate mobile charge carriers. Besides electronic conductance, doped conjugated polymers also mediate ionic conductance when interfaced with wet biological tissues due to the presence of ionic moieties. The three-dimensional micro/nanoporous polymer structure increases the surface area for electrostatic double-layer capacitive effect, resulting in volumetric contribution to the impedance at the interface, compared with a non-porous and pure metallic electrode (e.g., gold electrode). The ionic conductance originates from mobile ions (e.g., sodium, potassium ions or proton) transporting through the ionic medium containing ionic dopants (e.g., polystyrene sulfonate) and doped conjugated polymers (positive or negatively charged depending on whether p-doping or n-doping).[18] The mixed (both ionic and electronic) conductivity characteristic of conjugated polymers make them an ideal interface between ionic-mediated biological systems and electronic-mediated device circuits, offering reduced electrochemical impedance, higher current density, and higher signal-to-noise ratio.[19]–[21]

2.2. Chemical Tunability

There is abundant design space to chemically modify the side chains or conjugated polymer backbones to better mimic properties of biological systems. Self-healing,[22]–[24] degradable,[25,26] and biologically-responsive[27] properties can be introduced to conjugated polymers. Cell adhesion can be improved by various chemical and electrochemical methods, including functionalization of hydrophilic groups[28] (e.g., amine group) or arginylglycylaspartic acid (RGD) peptide[29] on conducting polymer side chain, selecting appropriate dopant (e.g., poly(2-methoxyaniline-5-sulfonicacid) (PMAS) and chondroitin sulphate (CS)[30]) and electrically switching conjugated polymer to partially reduced states.[31] In addition, the polymeric matrix can be chemically engineered to host biomolecules and drugs. For example, pharmaceutical drugs can serve as dopants in oxidized conjugated polymers and subsequently be electrochemically released.[32,33]

2.3. Biomechanical Compatibility

Localized (bidirectional) signal communication with high temporospatial resolution requires a soft and stretchable electronic interface, because interfaced biological tissues are viscoelastic, curvy, constantly moving and dynamic. Conjugated polymers with these properties have been designed to accommodate these unique features of biological tissue. By engineering Young's modulus, intrinsic stretchability, and other mechanical properties of conjugated polymers (Young's modulus ≈ 100s MPa-GPa) and especially electrically conductive hydrogels (Young's modulus ≈kPa), the large mechanical mismatch that exists between conventional rigid electronics (Young's modulus ≈GPa – TPa) and biological tissue (Young's modulus ≈kPa) can be closed.[34,35] As a result, the biomechanical compatible biointerface preserves the biomechanical microenvironment and can reduce or even eliminate immunoresponse and scar tissue formation, which are common problems in current clinically implanted electronics.[36]–[38]

3. Intracranial Neural Interface

Different from scalp-recorded electroencephalography (EEG), intracranial electrodes direct interface with brain tissue underneath the skull. As one of the most commonly used neural interfaces for both clinical and research purposes, intracranial electrodes show promise in regaining motor function,[39] memory,[40] sensory function[41] and recently, speech ability.[42] In clinical practice, epilepsy, especially drug-resistant epilepsy (accounting for one-third of total epilepsy cases[43]) requires implantation of intracranial electrode arrays for electrophysiological recording and stimulation. Electrophysiological recording with intracranial electrode arrays identifies the epileptic zone for subsequent removal; at the same time, microstimulation assist functional mapping of eloquent cortical region to avoid surgical damage. Intracranial electrode arrays take different form factors for electrocorticography (ECoG) and stereotaxic EEG (sEEG). ECoG electrode grids are thin membranes with a two-dimensional surface that are implanted on the brain surface in the subdural region (e.g., for epilepsy), while sEEG electrodes are often thin wires that are inserted deep into the brain, in order to record or stimulate deeper brain tissues (e.g., for Parkinson's disease).[44]

3.1. Accommodating Irregular Shape and Curvilinear Cerebral Cortex

The human cerebral cortex undergoes gyrification and forms ridges (i.e., gyrus) and depressions (sulcus). Each gyrus has a size[44] of ≈6 cm^2. The highly irregular and curvilinear surface creates difficulty for conventional rigid electronics and requires a flexible electrode array to form an intimate interface. Typical

thin plastic substrates (tens of micron meters) such as polyimide and evaporated metal interconnects allow relatively low bending radii and can, only to a certain degree (Intrasulcal space remains a challenge to access without delicate microdissection due to its deep structure[45]), conform with the gyrus for ECoG and microelectrocorticography (μECoG). The conducting polymer PEDOT:PSS can be readily electropolymerized on the metal (e.g., gold) to form a flexible thin-film form factor for direct electrochemical interfacing to the brain cortex.[46,47] The thickness of encapsulated devices, including conducting polymer and insulation layers, can be reduced to around 10 μm to decrease the bending stiffness, which is proportional to the inverse cube of thickness.[46,48] Lee et al. developed a ultraflexible ECoG electrode array with thickness of only 2.6 μm. The electrode array were arranged in a honeycomb mesh to allow structural stretchability.[49] Besides structural (e.g., shape and dimension) engineering, researchers have developed bioelectronics with soft polymeric materials as an alternative approach to conform with curvilinear surface of the brain. Blau et al. fabricated an all-polymer multielectrode array with PEDOT:PSS and graphite-polydimethylsiloxane (PDMS) as conductor.[50] The soft electrode array successfully recorded local field potential (LFP) responses to patterned visual stimuli in vivo on primary visual cortex of rats.

3.2. Shrinking Electrode Area Requires Lower Impedance

Missing important epileptic areas during EcoG mapping happens due to low electrode density, which gives relatively large interelectrode space. As a result, seizures cannot be eradicated in many epilepsy surgeries.[51] A large electrode area also diminishes the heterogeneity of local neural activity and leads to attenuation of high-frequency signals, such as high-gamma signals (originated from non-oscillatory synaptic activity) and abnormal high-frequency oscillations (HFOs), which are important for identification of seizure foci.[52]

Reducing the electrode size and increasing the electrode density (the number of electrodes per unit area) will allow more localized identification of neural activity (e.g., HFOs) for physicians, but, at the same time, pose the challenge of higher electrochemical impedance, because the impedance of non-porous electrode materials (e.g., platinum) is inversely proportional to the geometrical size. Unlike electrophysiological recordings in research labs, where electrical noise is well-controlled (e.g., with use of Faraday cages), ECoG recording in surgical rooms suffer from extensive electromagnetic noise from other essential medical equipment and therefore requires especially low electrochemical impedance. For a conventional (clinically-used) electrode with a size of ≈2 mm and an inter-electrode spacing of 1 cm, the impedance can be kept below kilo-ohm levels. With the same metal-based electronic materials, the impedance (at 1000 Hz) goes up to mega-ohm levels if one reduces the electrode size to be comparable to the size of a single neuron (≈20 μm).

Coating the metal electrode with additional layers of conducting polymer is an effective way to decrease impedance. Abidian et al. reported that the impedance of the electrode reduced by two orders of magnitude at the electrophysiological-relevant frequency of 1000 Hz after modification with poly(3,4-ethylenedioxythiophene) (PEDOT)-based materials.[53] To further reduce the electrode size, Khodagholy and co-workers demonstrated NeuroGrid[54] that recorded EcoG signal with an electrode size of 10 μm (**Figure 2**A). The free-standing PEDOT:PSS microelectrodes were lithographically patterned using paralyene as a sacrificial layer.[55] The impedance of NeuroGrid electrodes (≈$2\times10^{[4]}$ Ohm) was more than ten times lower than that of gold electrodes or silicon probes. Because the electrode size matched that of neuronal bodies, it was shown to record both local field potentials and putative single-unit action potentials without the need for brain penetration in two human patients during epilepsy surgery (Figure 2B). In a separate study,[56] PEDOT:PSS electrodes (Figure 2C) with slightly larger areas (e.g., 50 μm in diameter) were unable to record action potentials, highlighting the importance of using high-density and high spatial resolution electrode arrays. Nevertheless, the conducting polymer-coated electrode was capable of recording stimulus-locked cognitive activity within a distance of 400 μm. Besides, the device recorded a noticeable increase in epileptiform activity 200s after administration of Methohexital, a drug that is known to induce seizures (Figure 2D). The PEDOT:PSS maintained its mechanical and electrochemical performance after autoclave sterilization, an essential step for clinical application. Recently, a clinical study (Figure 2E) involving 30 human participants demonstrated reliable intracranial monitoring by PEDOT:PSS microelectrodes during surgical resection.[57] The low impedance electrode could record unitary events that can be specifically modulated by different external stimuli.

How do conducting polymers like PEDOT:PSS substantially reduce electrochemical impedance to form a low impedance interface with ionically-conductive tissue? Many doped conjugated polymers exhibit mixed conductor properties. That means the conducting polymer electrode can be modeled as having both a capacitor and a resistor in parallel. At lower frequency, the capacitive contribution, especially from the porous nature of the conducting polymer can help to significantly reduce the overall impedance at the interface (Figure 2F). This makes them ideal for direct interfacing with biological systems.[58,59]

3.3. Exploiting High Transconductance of Conjugated Polymer Based Electrochemical Transistor

The drain current in organic electrochemical transistors (OECT) can be controlled by the injection of ions into conjugated polymers, owing to their mixed conduction and high ionic mobility.[18] Khodagholy et al. reported that OECTs had superior signal-to-noise ratio compared to conventional surface electrodes[60] (**Figure 3**A). PEDOT:PSS was used as semiconducting channel, and a noble metal was used as the source and drain. The high transconductance (900 μS) of the PEDOT-based OECT[61] amplified the small potential on the brain surface (in the range of μV). The PEDOT-based OECT demonstrated superior signal-to-noise ratio for recording of surface low-amplitude brain activities, which were poorly resolved with surface electrodes (Figure 3B).

ECoG mapping of drug-induced epilepsy in vivo showed local field potential (summation of a group of neural activity), but single-unit-like electrophysiological signals were not observed, although the electrode size used was comparable to that of

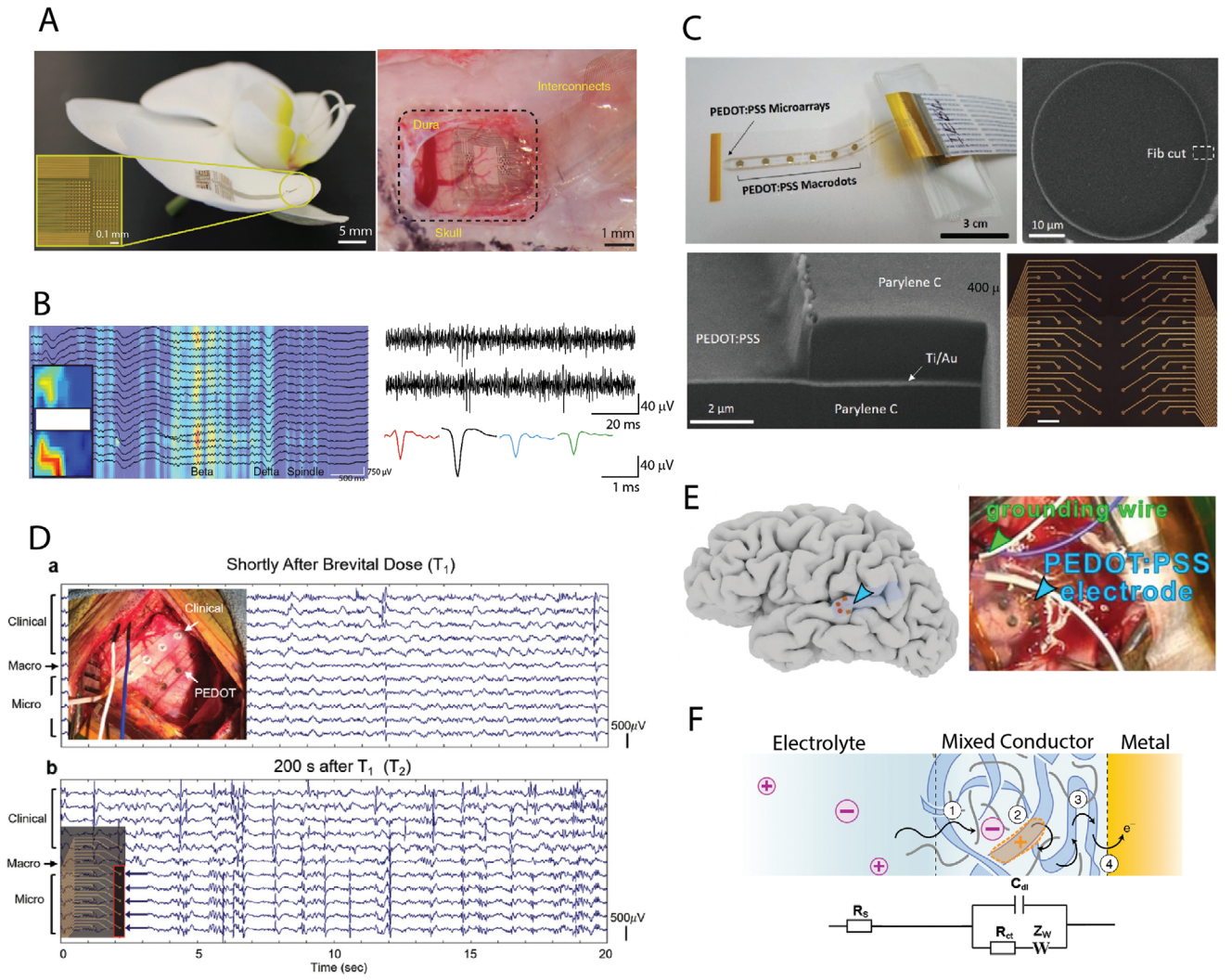

Figure 2. Conducting polymer based ECoG Electrodes. A) PEDOT:PSS electrode array NeuroGrid conforms to a curved surface and rat somatosensory cortex. B) Time-frequency spectrogram and Intraoperative recording of both local field potential (LFP) and spikes in epilepsy patients. Reproduced with permission.[54] Copyright 2015, Nature Publishing Group. C) PEDOT:PSS electrophysiology device on thin-film parylene C layer with conformal and intimate contact between the different layers. D) Simultaneously captured ECoG traces from clinical, PEDOT macro, and micro electrodes before and 200 s after epileptiform-inducing Methohexital. Reproduced with permission.[56] Copyright 2018, Wiley-VCH GmbH. E) PEDOT:PSS record on the surface of the human cortex. Reproduced with permission.[57]Copyright 2021, Oxford University Press. F) Charge transport in conjugated polymer as a ionic-electronic mixed conductor 1) dopant ion injection; 2) electronic carrier (hole) stabilization by a dopant ion (anion); 3) electronic carrier hopping, and 4) charge transfer between the metal electrode and the mixed conductor. The electrochemical impedance can be modelled by Randles circuit, where R_s, C_{dl}, R_{ct}, and Z_w are electrolyte resistance, double layer capacitance, charge transport resistance, and Warburg element. Reproduced with permission.[59] Copyright 2020, Nature Publishing Group.

Neurogrid. One possible reason can be that the response speed of traditional OECTs is not fast enough to accommodate millisecond-scale action potentials.[62] In such cases, one can only back-calculate the voltage by using complicated modeling with known device parameters, which is impractical in clinical applications. More recently, the enhancement-mode, internal ion-gated organic electrochemical transistor (e-IGT) developed by Cea et al. demonstrated high operational speed with a short rise time of 2.9 μs while maintaining ≈1.5mS transconductance[63] (Figure 3C). When the device is in the "off" state, the amine group on polyethylenimine (PEI) transfers electrons to PEDOT:PSS, forming $PEDOT^0$. Once the gate voltage becomes negative, PEI^+ is compensated and PSS^- re-dopes the PEDOT, leading to a dramatic increase of channel conduction. Action potentials were successfully recorded in freely moving epileptic rats with improved response time. Compared with microelectrodes, the key advantage of using an electrochemical transistor is that it can locally amplify the signal, which improves the signal quality, especially when long interconnects are used or an electrically noisy environment is present (Figure 3D). In addition, an active OECT matrix can reduce the number of interconnecting wires by (N×M)-(M+N), where N and M are the number of rows and columns,

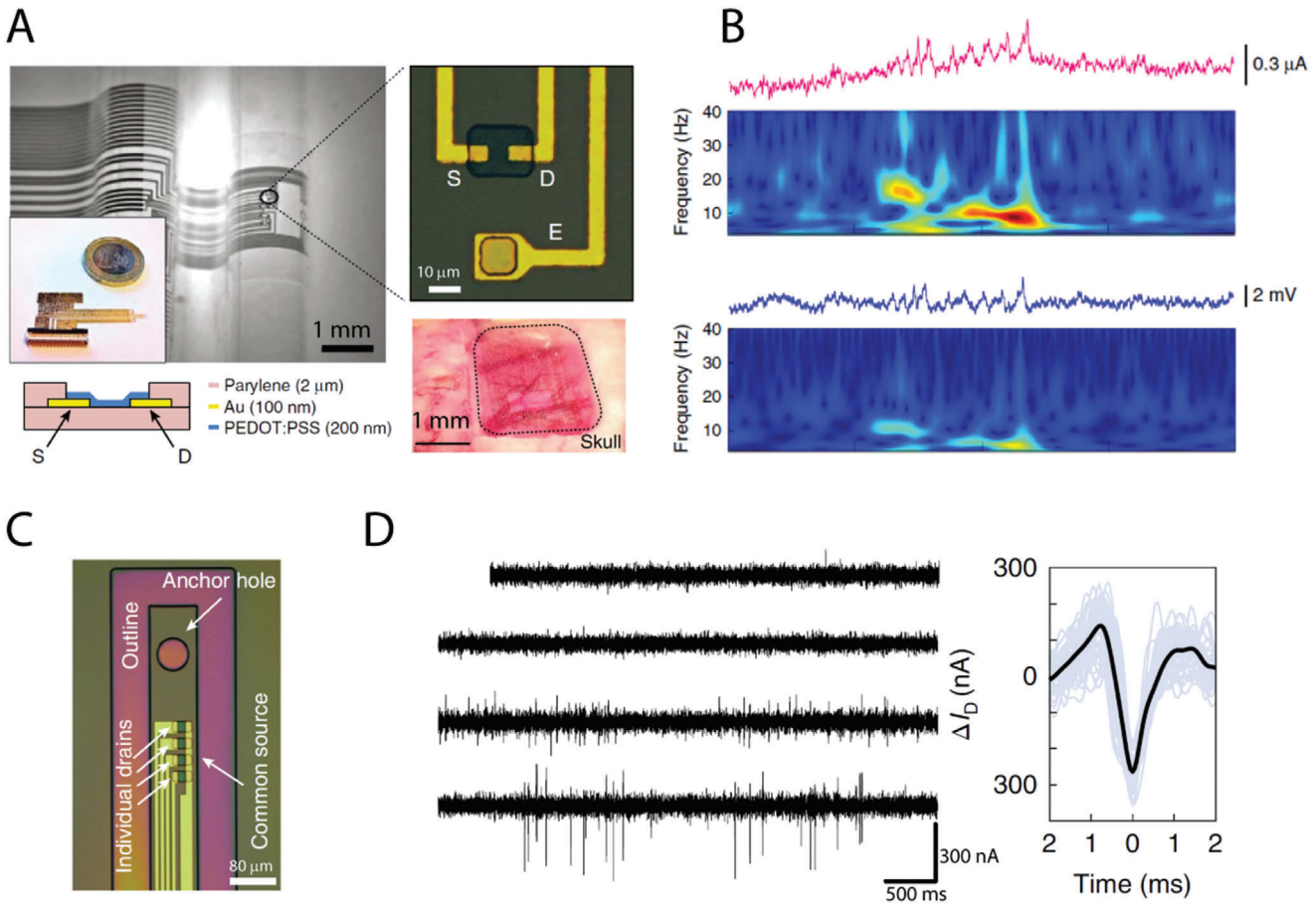

Figure 3. Organic electrochemical transistor neural probes. A) OECT EcoG probe conforms to curvilinear surface and somatosensory cortex. B) The OECT recording and time-frequency analysis plot showed higher signal resolution for PEDOT:PSS based OECT (top) compared with an a PEDOT:PSS surface electrode (lower). Reproduced with permission.[60] Copyright 2013, Nature Publishing Group. C) Optical micrograph of an e-IGT-based device with four transistors for LFP and spike recording. D) High-pass filtered traces (250–2500 Hz) from four e-IGTs in deep layers of rat cortex revealing waveforms suggestive of neural action potentials. Trigger averaging of waveforms demonstrated consistent action potential morphology. Reproduced with permission.[63] Copyright 2020, Nature Publishing Group.

respectively.[64] This is important to reduce the number of interconnects needed for large-scale high-density electrophysiological mapping. As a powerful alternative to microelectrodes, it has the potential to be tested and deployed for intraoperative ECoG in hospitals in the near future.

3.4. Conjugated Polymer-Based Penetrating Electrodes with Reduced Immunoresponse

Penetrating electrodes are needed to access epileptic regions hidden in the deep cerebral cortex and for deep brain stimulation to treat neurological disorders. Compared with EcoG electrodes, penetrating electrodes are advantageous for capturing single-unit neural activity due to the proximity of the electrode to individual neurons. At the same time, penetrating electrodes are more invasive and pose a higher risk for adverse immunoresponse, especially for nervous tissues. After neuroelectronic implantation, glial cells, including microglia and astrocytes, can be activated by blood-serum proteins due to the disruption of the blood-brain barrier. Microglia upregulate proinflammatory cytokines that leads to neurodegeneration. The activated astrocytes and microglia encapsulate implanted devices by forming a dense scar tissue around them. The astroglial reactivity increases the expression of connexon (CX43) that further promote the inflammation in the nearby tissue. Reducing the electrode size and stiffness has shown to reduce the immunoresponse by preventing the activation of astrocytes, reducing the upregulation of inflammatory signaling (e.g., TNFα and IL-1β) and avoiding injury to blood-brain-barrier.

Electrochemical deposition at the cross-sectional surface of ultrathin substrates formed edge electrodes.[65] Not only can edge electrodes be made into small sizes, but they also increase the volume of electrophysiologically-recorded tissue with electrophysiological access to neurons on both sides of the thin-film substrates. It was demonstrated that gold electrodes with electrochemically deposited PEDOT maintained stable electrochemical performance when subjected to electrophysiological conditions (aqueous environment at 37 °C) for 60 days. The PEDOT-based electrode array could be scaled to 1024 channels and record 375

single-unit activity in freely behaving rats[66] (**Figure 4**A). Bodart et al. reported that a PEDOT-coated deep brain stimulator (DBS) increased the charge storage capacity and operated in vivo for 2 weeks with daily stimulation[67] (Figure 4B). EDOT-acid can improve the adhesion between metal and conducting polymer and has the potential to further increase its aqueous stability.[68] For chronic implanted electronics such as DBS, the penetrating electrodes ideally should be stable in physiological condition for more than 5 years, which remains a challenge for conjugated polymer. Longer term in vivo evaluation of conjugated polymers is needed before translating them into clinical applications.

The human brain is dynamic due to locomotion and cardiorespiratory cycles, and the micro-motion leads to signal drift and instability in the brain-machine interface.[69] Flexible electrodes can potentially reduce the effects of micro-motion. The immunoresponse due to mechanical mismatch between electrodes and electrogenic tissue also presents a great challenge for chronic biointerrogation.[70] Glial response to stiff electrodes leads to insulating scar tissue formation around electrodes.[37] Reducing bending stiffness with structural design is one potential way to reduce immunoresponse. Neurolink Co. developed a suture-like neural probe with high bandwidth.[71] Bending stiffness mismatch between neural tissue and PEDOT coated electrodes (Figure 4C) were reduced due to its ultrathin (≈5 μm) structure and low thread width (5-50 μm).[71] Surface modification with PEDOT:PSS resulted in a lower impedance and higher charge-carrying capacity when compared with IrOx modification (Figure 4D). 3000 electrodes on the threads were inserted in a rat brain with the assistance of an advanced robotic system for simultaneous recording (Figure 4E).

Another way to combat immunoresponse is to engineer the Young's modulus of the neural interface. Despite the challenge in developing soft electronic materials and fabrication processes, engineering the intrinsic properties of electronic materials allows more freedom in the geometry and design of the electronics. Especially, handling a thin film or thread-like device with 5 – 10 μm thickness during surgical implantation is challenging for most neurosurgeons. A slightly thicker (e.g., ≈50 μm) device with tissue-like Young's modulus offers better clinical practicability. Coating electrodeposited PEDOT:PSS (Young's modulus: ≈ 2.6 GPa) with ionically conductive (not electrically conductive) alginate hydrogel (Young's modulus: ≈ 30 kPa) can reduce the mechanical mismatch.[72] While alginate hydrogels offer improved mechanical compliance and biocompatibility, they also reduce the neural recording signal. In fact, the average percentage of detectable unit drops linearly as the alginate hydrogel thickness increases. To avoid the trade-off between signal quality and biomechanical compatibility, the design concept of promoting an interconnected conduction pathway or network inside a soft matrix have been most effective. For example, Feig and coworkers developed a dual conductive (i.e., both ionic and electronic conductive) hydrogel. The interpenetrating network hydrogel had a conductivity of 23 Sm^{-1}. Notably, the mechanically tunable Young's modulus allows researchers to match with that of interfaced electrogenic tissue.[35] By using a ionic liquid to induce aggregation of PEDOT, Liu et al. further developed a PEDOT:PSS hydrogel with Young's modulus in the range of kilopascal (comparable to that of neural tissue), while achieving a high electrical conductivity of 4700 Sm^{-1}. Based on the unique anisotropic swelling-deswelling of the pure PEDOT:PSS hydrogel, a hydrogel electrode array with a feature size of 20 μm was fabricated.[34] Zheng and co-workers combined geometry design and modulus engineering to further improve the biocompatibility profile of implantable electronics. They developed a PEDOT-PEG copolymer-based suture electrode (diameter of ≈100 μm) with Young's modulus below 1 MPa.[73] Taking together a high aspect ratio and relatively low Young's modulus, the suture electrode showed excellent biocompatibility and had a desirable form factor to integrate into the daily practice of clinicians.

4. Peripheral Nerve Electronic Interface

4.1. Localized and Low-Voltage Neuromodulation

Extra-neural electrodes are less invasive compared to interfascicular or interfascicular electrodes and therefore are often used clinically for vagus nerve or sacral nerve stimulation.[74] Electrode (array) cuffs typically wrap around tubular-shaped nerves to form a tight interface. Although the substrate and encapsulation of cuff electrodes are made up of soft elastomers, such as PDMS, their electrode materials, such as platinum or platinum-iridium, are usually rigid.[75] Qi et al. reported a conducting polymer polypyrrole (PPy) electrode that provided a stretchable sciatic nerve interface using a pre-stretching strategy.[76] The PPy nanowire sustained over ten thousand stretch-release cycles without significantly compromising electrical performance. The relatively large electrode size and lack of top encapsulation limited its application for localized neuromodulation. Liu et al. overcame this challenge by developing a lithographically micropatterned, fully encapsulated stretchable microelectrode using an electrically conductive PEDOT:PSS hydrogel[34] (**Figure 5**A). In order to accommodate sciatic nerve movement during stretching of the leg, both the electrode and interconnect were designed to be soft (Young's modulus ≈ 20kPa) and stretchable. Electrically conductive hydrogel was used for both interconnects and electrodes. Different from metal interconnects, nanoporous polymer interconnects made of conducting polymer further reduces the impedance when compared with conducting polymer-coated metals[77] (Figure 5B), which can be modeled by a modified transmission line equivalent circuit.[34] Interconnect architecture, besides electrode dimension, can be used to modulate electrode properties for designing clinical electrodes. Leveraging the dual conductivity in both electrodes and interconnect, the hydrogel-based neural interface gave 30 times higher current injection density compared with platinum electrode of the same size. In addition, an ultralow voltage of 50 mV was sufficient to elicit leg movement upon stimulation on the sciatic nerve. Low-impedance polymeric electronics have the potential to be used for VNS to treat drug-resistant epilepsy and to modulate inflammation reflex[78] and the brain-gut axis.[79]

4.2. Regenerative Nerve Guidance Conduit

Abundant free volume in the conducting polymer matrix allows electrolyte to diffuse in. Their mixed conductive nature and excellent biomechanical compatibility make conducting polymers an ideal candidate for functional nerve scaffolds, where

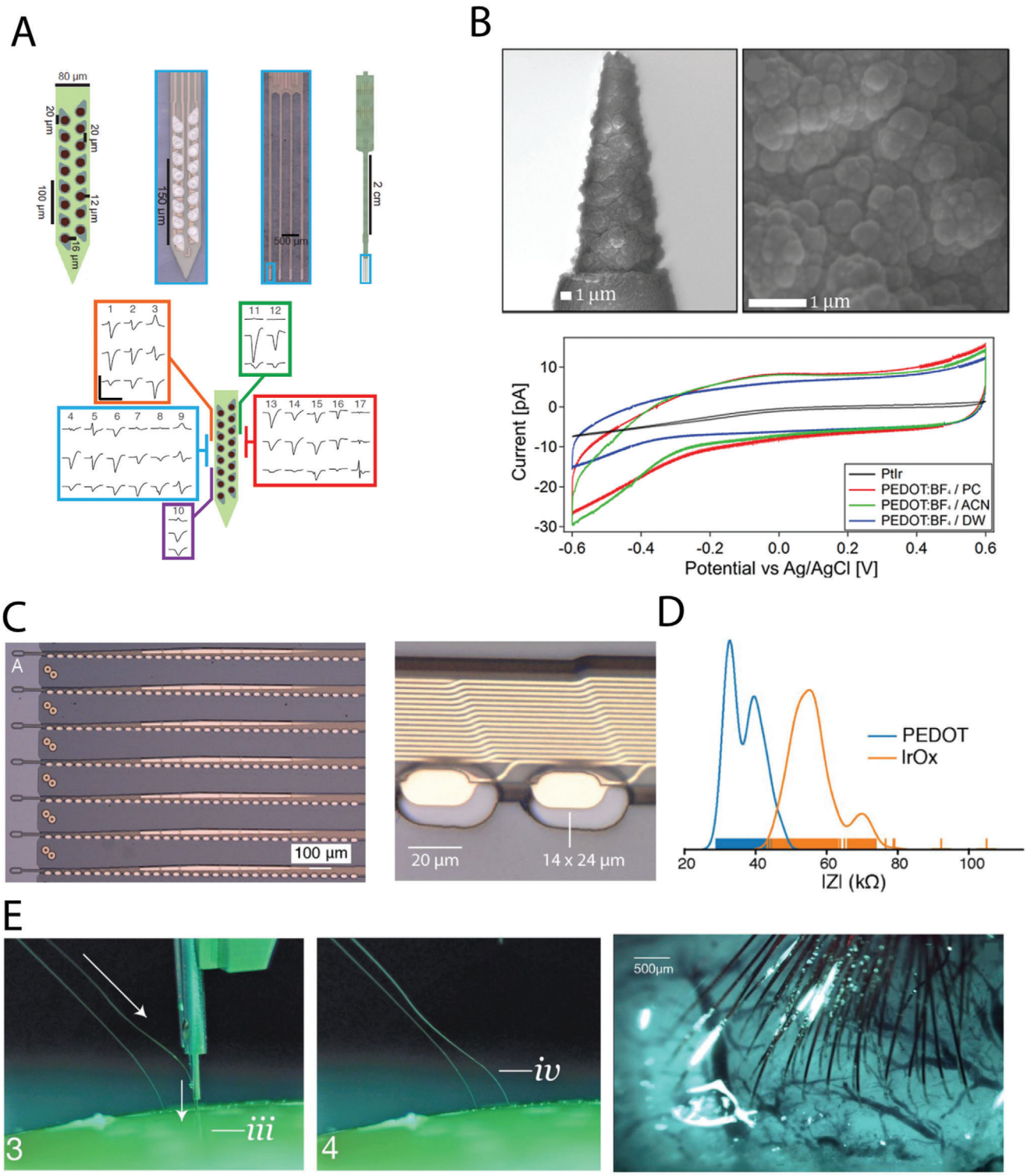

Figure 4. Conducting polymer functionalized penetrating microelectrodes. A) Electrochemically polymerized PEDOT electrode array. Stable and well isolated single-unit recording after 160 days of implantation. Reproduced with permission.[66] Copyright 2019, Elsevier. B) PEDOT:BF4 galvanostatically electropolymerized on PtIr electrode for deep brain stimulation. Cyclic voltammetry (CV) showed enhanced charge storage capacity for PEDOT-coated recording microelectrodes compared with uncoated ones. Reproduced with permission.[67] Copyright 2019, American Chemical Society. C) Flexible thread-like electrode array with high density (32 electrode contacts spaced by 50 µm). D) Distribution of electrode impedances (measured at 1 kHz) for two surface treatments: PEDOT ($n = 257$) and IrOx ($n = 588$). PEDOT coating yielded a lower electrode impedance compared with IrOx coating. E) Implantation procedure for thread-like flexible electrode array. Multiple threads can be implanted at customized depth with assistance from automated needle penetration. Reproduced under Creative Commons Attribution License.[71] Copyright 2019, the Author(s). Published by JMIR Publications.

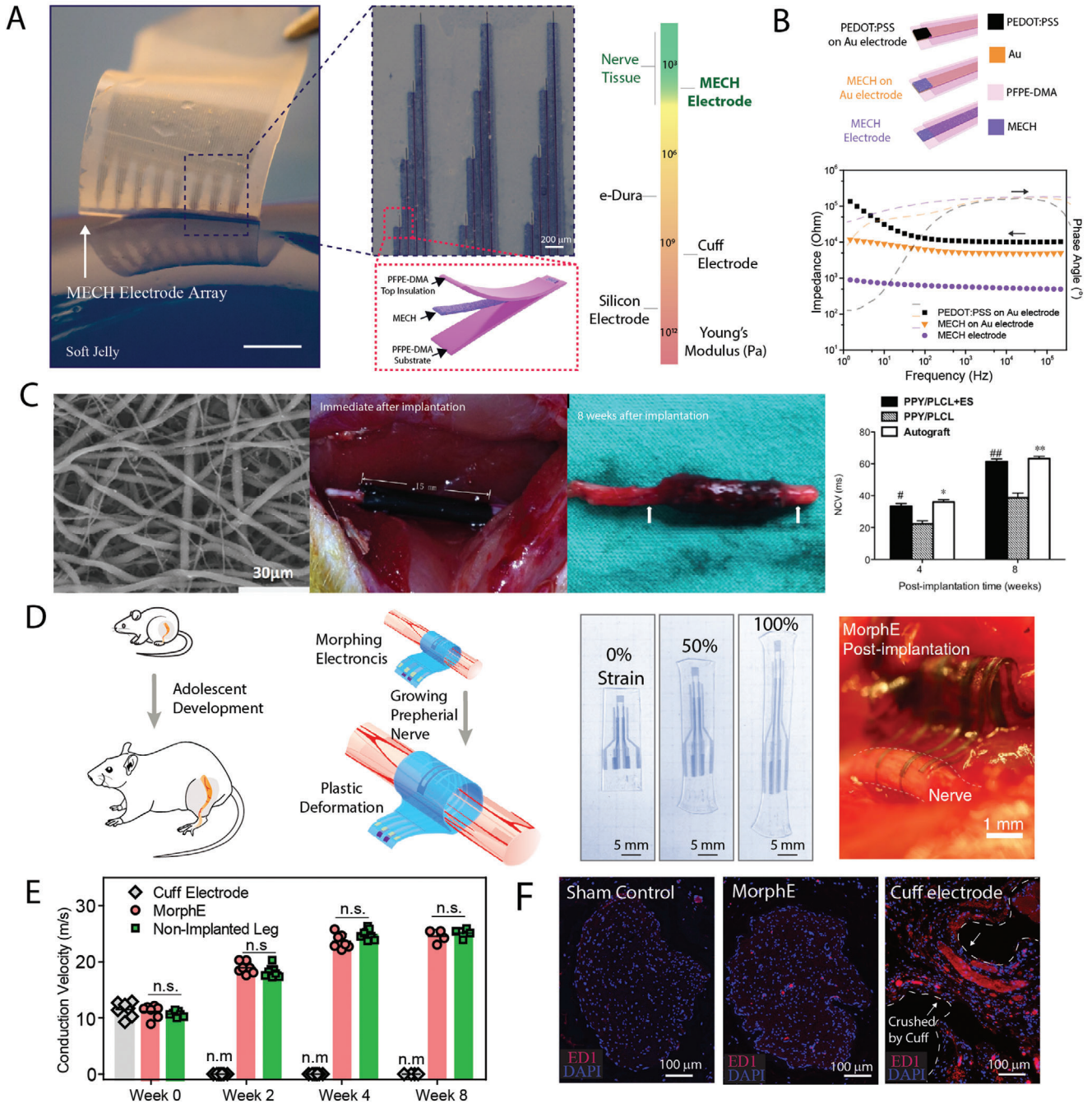

Figure 5. Soft peripheral neural interface. A) Lithographically patterned hydrogel (MECH) elastronics with Young's modulus comparable to that of nerve tissue. B) MECH electrodes (MECH as both interconnect and electrode) had substantially low electrochemical impedance compared with PEDOT:PSS or MECH coating on metal electrode. Reproduced with permission.[34] Copyright 2019, Nature Publishing Group. C) 15 mm gaps of sciatic nerves were bridged using electrical stimulation of polypyrrole (PPy)/PLCL nanofibers based regenerative nerve conduit. Reproduced with permission.[82] Copyright 2016, Frontiers Media S.A. D) Morph electronics (MorphE), made of viscoplastic electronic materials, conformally adapts to sciatic nerve growth in vivo. E) Rats implanted with MorphE had similar conduction velocities to nonimplanted nerve from week 0 to week 8 post-implantation, while cuff electrode failed after 2 weeks of implantation due to tissue outgrowth. F) MorphE-implanted nerve had similar level of ED1 (a marker for inflammatory response) expression compared with sham control. Chronic compression resulted from non-adaptive cuff electrode led to high expression of ED1. Reproduced with permission.[90] Copyright 2020, Nature Publishing Group.

conducting polymers not only provide an immediate microenvironment for cells, but also provide chronic electrical stimulation. PPy nanofiber-based scaffolds provided a high Faraday current density for direct current stimulation.[80] Song et al. showed that electrical stimulation of human induced stem cell-derived neural progenitor cells led to upregulation of neurotrophic factor expression, which is important for synaptic remodeling and nerve regeneration.[81] Direct current stimulation using a PPy/PLCL nerve conduit induced nerve growth and functional recovery on a sciatic nerve with large (15 mm) defect (Figure 5C).[82] It had similar performance compared with autograft and was significantly better than a non-stimulated conduit.

An ideal nerve guide should disintegrate and biodegrade after nerve regeneration. Biodegradable polymers, such as poly(Llactic acid-co-ϵ-caprolactone)(PLCL)[82] or poly(L-lactide)[83] were typically mixed with polypyrrole, followed by electrospinning into nanofibers. However, the conducting polymer was not degraded in those cases. Imine bonds are conjugated linkages that can be broken down in weakly acidic environments, and thus can be explored as a potential method to develop biodegradable conjugated polymers.[84] Alternatively, water-soluble conducting polymers such as poly[ammonium- (3-thienyl)ethoxypropanesulfonate] (SPT)[85] can be used to construct bioerodible devices that break down into polymers with molecular weights lower than the renal filtration threshold, i.e., 30 kDa. For more examples, readers can refer to comprehensive reviews[86,87] regarding nerve regeneration with conducting polymers.

4.3. Growth-Adaptive Conjugated Polymer for Pediatric Electronic Medicine

Human growth has largely been overlooked for current bioelectronics development, partly because of the lack of available electronic materials. Young children implanted with devices like VNS suffer from severe tissue constraints and functional damage as they grow.[88,89] Liu et al. developed a system of growth-adaptive soft electronics named "morphing electronics" or MorphE[90] (Figure 5D). A viscoplastic conductor made from PEDOT:PSS and glycerol could be permanently deformed by the strain from tissue growth and thus maintained a seamless interface throughout adolescent development. Morphing electronics caused minimal damage to the rat nerve and allowed chronic electrical stimulation and monitoring for 2 months without disruption of functional behavior (Figure 5E). In contrast, commercial cuff electrodes cause permanent damage due to chronic compression (Figure 5F). Although the authors only demonstrated the concept of MorphE in the peripheral nervous system, the general strategy of developing viscoplastic electronics can be applied widely to other pediatric implantable devices. Additional viscoplastic electronics materials, such as bioresponsive, dielectric, semiconducting materials can be further added into the library of morphing electronics to enable multimodal functionalities for pediatric electronic medicine. It is important to develop electronic medicine that is sensitive to the biology of growing children, rather than treating children as adults with smaller body size. The new research area in growth-adaptive implantable electronics can solve this long-standing problem in the pediatric population and lead to next-generation pediatric electronic medicine.

5. Cardiac bioelectronic Interface

5.1. Accommodating a Constantly Moving Organ

Electrical rotors and focal impulses are proposed to be the key drivers of atrial fibrillation. Electrophysiological mapping of those irregular electrical activities and subsequent accurate identification of their spatial location enables patient-specific ablation, offering high efficacy and fast treatment.[91] Conventional basket electrodes have low spatial resolution in centimeter scale and do not accommodate with heart beating. Seamless mechanical coupling on a beating heart and high-spatial-resolution mapping are the two challenges that stretchable conducting polymers are uniquely suited to address. Inorganic electrode arrays have demonstrated electrophysiological mapping in an *ex vivo* experiment using a wavy structure design.[92] Intrinsically stretchable devices using elastic conducting polymer, on the other hand, offer more compact interconnect packing and therefore improve the electrode density. Cardiac activities were recorded by an all-polymer electrode array[50] on an extracted embryonic mouse heart. Although global ECG-like electrical signals were recorded, localized signals were not observed due to the large electrode size of 0.5 mm. Taking advantage of lithographical micropatterning, an intrinsically stretchable PEDOT:PSS microelectrode with electrode size of 80 μm was developed[93] (**Figure 6**A,B). The stretchable array was used for epicardial mapping (on atria) in chronic atrial fibrillation porcine model in vivo. The thin-film stretchable device mechanically coupled with the dynamically beating heart and gives stable electrophysiological recordings. Compared with the state-of-the-art endocardial-mapping techniques, the epicardial mapping with stretchable organic microelectrodes gave 2 times higher atrial-to-ventricular signal ratio and >100 times higher spatial resolution. It is worth noting that electrical local heterogeneity in chronic atrial fibrillation was identified thanks to its cellular-level spatial resolution.

5.2. Passive Conductive Constructs to Bypass Impaired Cardiac Tissue

Cardiac disease such as myocardium infarction or neuromuscular disorder causes cellular death and fibrosis, which impair the normal conduction pathways between cardiomyocytes. The lack of electrical communication between cardiomyocytes further leads to arrhythmia and asynchronous contraction. A conductive polymer patch with high ionic mobility can provide a low-impedance interface between cardiomyocytes and bypass insulating scar tissues.[94] The ion mobility within a conjugated polymer scaffold is higher than that in solution due to the contribution of electro-osmosis in the conjugated polymer network.[18] Self-doped conductive polymer (poly-3-amino-4- methoxybenzoic acid, PAMB) had 30 times higher conductivity compared with gelatin-based Gelfoam (a commercial product).[95] As a result, the PAMB epicardial patch significantly increased electrical impulse propagation and synchronic cardiomyocyte contraction across the scar region. Mawad et al. improved the stability of Polyaniline (PANI) by utilizing the strong chelation between the dopant phytic acid and chitosan substrate.[96] The PANI patch increased the conduction velocity on the infarcted heart in an *ex vivo* experiment (Figure 6C). Polydopamine can be used as

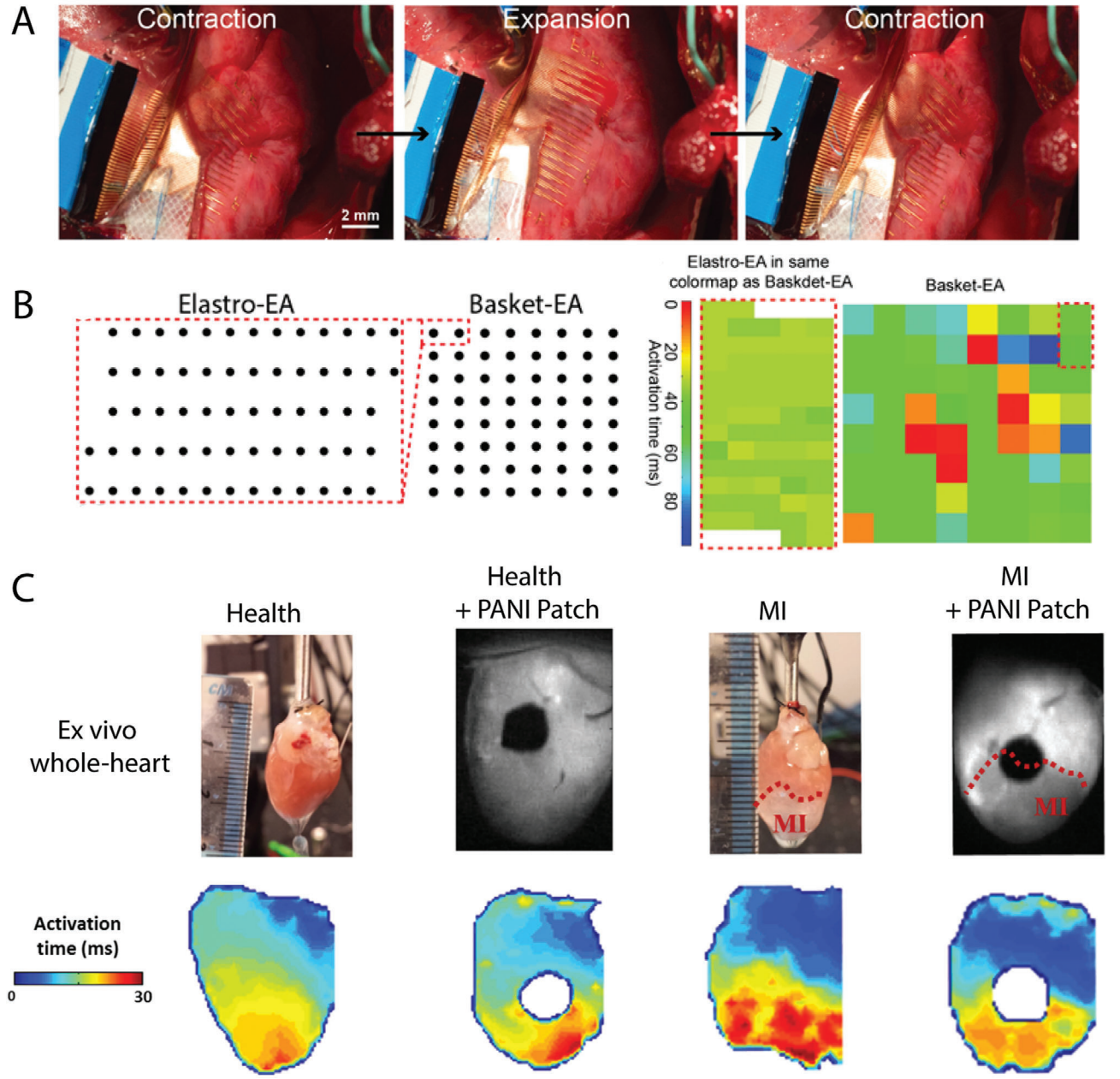

Figure 6. Active and passive cardiac interface with conducting polymer. A) Intrinsically stretchable electrode array effectively prevented sliding and delamination from the epicardial surface during expansion/contraction of the right atrium in porcine with chronic atrial fibrillation. B) Isochronal maps of activation time from endocardial basket electrodes and the epicardial elastrode array from the same temporal reference and scale. High-density elastrode detected localized electrical heterogeneity within the 10- to 30-ms time scale that can not be resolved using conventional clinical electrode array. Reproduced with permission.[93] Copyright 2020, PNAS. C) Representative activation time before and after PANI/Chitosan conductive patch application on healthy control hearts and on hearts 2 weeks after MI The electrically conductive patch increased conduction velocity in the apical infarcted area. Reproduced with permission.[96] Copyright 2016, American Association for the Advancement of Science (AAAS).

a wet adhesive for the conductive polymer-based cardiac patch for improved stability on a dynamically moving heart.[97] The conductive polymer could also be made into an ink form for printing directly onto cardiac tissue. By in situ polymerization of polypyrrole and dopamine in presence of Fe^{3+}, the printable polymer rapidly formed bonds on the wet epicardia surface. The cardiac patches promoted reconstruction and revascularization of the infarct myocardium.[98]

6. Biomolecular Interface for Chronic Diseases

Implanted drug delivery platforms are a promising way to address biochemically-treatable chronic disease, as the possibility for localized delivery can help mitigate off-target or large-dose effects from systemic administration. Implanted platforms that have achieved clinical translation so far rely on passive processes like diffusion to deliver drugs; however, researchers are

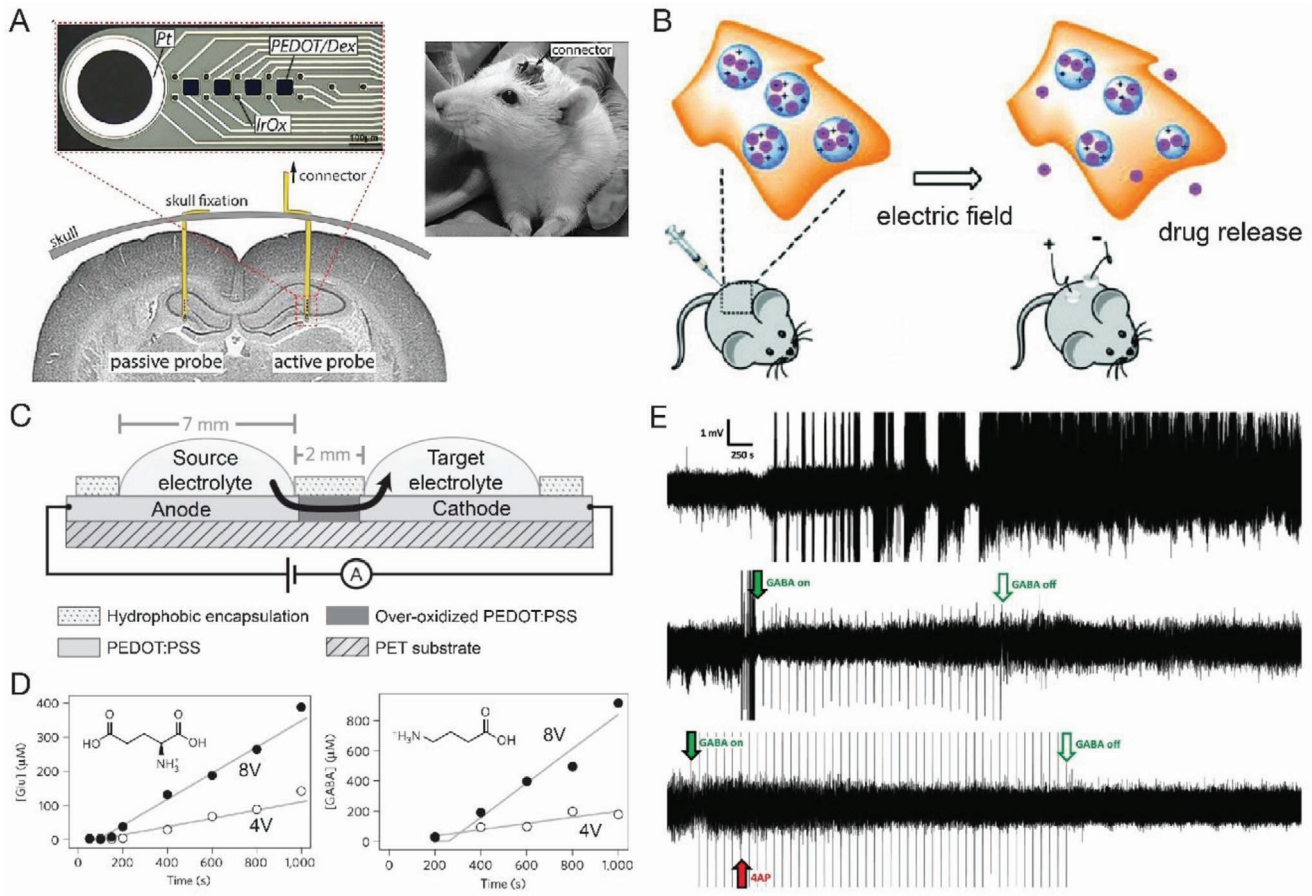

Figure 7. Conducting polymer-based devices for active drug delivery. A) Flexible neural microelectrodes comprising PEDOT:PSS doped with the anti-inflammatory drug Dexamethasone, which was released on-demand after implantation into a rat hippocampus. Reproduced with permission.[32] Copyright 2016, Elsevier. B) PPy nanoparticles loaded into an injectable hydrogel can encapsulate charged small molecule drugs with high loading, with release triggered by application of an electric field. Reproduced with permission.[100] Copyright 2012, American Chemical Society. C) Side view of an organic electronic ion pump (OEIP) with over-oxidized PEDOT:PSS as the drug-selective membrane. D) The OEIP enables voltage-dependent delivery of neurotransmitters Glu and GABA. Reproduced with permission.[104] Copyright 2009, Nature Publishing Group. E) Electrophysiology recordings showing seizure-like events (SLEs) (top), microfluidic ion pump delivery of GABA following SLE showing successful treatment (middle), and delivery of GABA to prevent SLE occurrence before prior to injection of 4AP. Reproduced with permission.[107] Copyright 2018, AAAS.

increasingly interested in leveraging conjugated polymers for active control of drug release, enabling dosing schemes like pulsatile or closed-loop drug delivery. A comprehensive study of recent advances in this space was published earlier this year.[99] Unfortunately, there are still no clinical studies of conjugated polymer-based implanted drug delivery platforms, in large part because of barriers associated with regulatory approval of new functional materials. Indeed, validation of most reported conjugated polymer-based drug delivery systems has been limited to in vitro demonstrations of efficacy. In this section, we will specifically highlight works that have also included in vivo validation, as they are furthest along the pathway to clinical translation.

6.1. Encapsulation and Release of Charged Small Molecule Drugs

Conjugated polymers can entrap charged drug molecules via electrostatic interactions, with subsequent release occurring either passively via diffusion or counter ion exchange, or in a controlled manner by applying electrochemical potentials to modulate the redox state of the conjugated polymers. Boehler and coworkers used this controlled approach to release dexamethasone (Dex), a charged anti-inflammatory drug, from flexible neural microelectrodes implanted in a rat hippocampus in order to test its ability to mitigate inflammation from the electrode insertion process[32] (**Figure 7**A). Iridum oxide (IrOx) microelectrodes were coated in PEDOT via electropolymerization, with Dex incorporated into the conjugated polymer film as a dopant during the polymerization step at 19 ng per probe. Dex was released on-demand from the PEDOT coatings by applying a cyclic voltammetry (CV) scan in a three-electrode configuration. 320 stimulation sessions were performed over the course of twelve weeks. While it is unclear whether the active delivery of Dex had a significant therapeutic impact, the study noted that CV stimulations could be done in fully awake animals without evoking reaction or inflammation in the histology. Notably, bare IrOx had the best performance compared to PEDOT-only, PEDOT/PSS, and PEDOT/Dex-coated electrodes, which was attributed to

residues from the PEDOT electropolymerization process. This surprising finding underscores the importance of accounting for the biocompatibility of different synthetic routes and potential impurities that may be introduced through manufacturing when designing conjugated polymer-based systems.

While drug encapsulation in conjugated polymer films may be sufficient for shorter-term delivery of highly potent drugs, larger doses or longer implantation times necessitate higher drug loading. One way to increase loading is to encapsulate drugs in conjugated polymer nanoparticles embedded within a hydrogel depot, though this potentially compromises on spatial control of delivery. Ge and coworkers used PPy nanoparticles to encapsulate either negatively or positively charged molecules, which could then be released with the application of a weak DC electric field to induce reduction or oxidation of the PPy, respectively[100] (Figure 7B). For in vivo applications, fluorescein-laden PPy particles were encapsulated at 1 wt% in a thermoresponsive PLGA-PEG-PLGA injectable hydrogel and shown to be biocompatible in mice. To test triggerable release, a voltage was applied between the particle injection site and a separate injection site. As expected, fluorescence from released fluorescein molecules was only observed after application of an electric field. While this is an exciting proof-of-concept and subsequent reports have shown that it is feasible to use conjugated polymer-based hydrogel depots to deliver therapies like anti-cancer drugs and insulin[101–103], in vivo demonstrations of therapeutic effect with these drugs are still needed.

6.2. Drug-Selective Membranes for Neurotransmitter Delivery

To simultaneously enable high drug loading capacity and high spatial control, organic electronic ion pumps (OEIP) that incorporate conjugated polymers as drug-selective membranes are increasingly being explored. In this design, drugs can be electrophoretically pumped across the conjugated polymer membrane from a separate reservoir, thereby decoupling loading capacity from the thickness of the conjugated polymer film, and high spatial control can be obtained by using microfabrication techniques to fabricate devices. Agneta Richter-Dahlfors and colleagues used photolithographic patterning to fabricate planar ion pump devices with PEDOT:PSS (Figure 7C) to deliver glutamate (Glu) in a voltage-dependent manner to the auditory system of guinea pigs[104] (Figure 7D). Glu is a neurotransmitter that is negatively charged at neutral pH and acts on inner hair cells of the cochlea to transduce sound waves. Shifts in the auditory brain response (ABR) threshold illustrated the effect of Glu in real time: after 60 minutes of continuous delivery, a statistically significant shift in ABR threshold was observed at all tested frequencies. Notably, excitotoxic swelling was observed in some inner cell dendrites, suggesting that better temporal control of delivery is desirable for this application. For future investigations, their platform could readily accomplish this by modulating the electrophoretic driving voltage with time, for instance using pulsatile instead of continuous release.

In the first demonstration of an organic electronic delivery device implanted into an awake and moving animal for therapeutic purposes, Johnsson et al. implanted a PEDOT:PSS-based OEIP device into the spinal cord of a spared nerve injury (SNI) rat model to locally deliver GABA, the primary inhibitory neurotransmitter in the central nervous system.[105] Implantation did not lead to any observable signs of spinal cord injury. Tactile hypersensitivity is a feature of the SNI model, and is characterized by unusually low threshold of applied tactile force needed to induce a brisk withdrawal of the hindlimb (withdrawal threshold, WT). Validating the therapeutic effect of drug delivery from the device, rats that received $GABA^+$ from implanted OEIPs showed significant increases in WTs compared to those that received H^+, which was used as the negative control.

Recently, a modified OEIP called a microfluidic ion pump (μFIP) was reported that simplifies the process of replenishing the ion reservoir, allowing for high drug loading over even longer implanted timescales.[106,107] Proctor et al. fabricated neural probes consisting of μFIPs to deliver the neurotransmitter GABA to the hippocampus as a therapeutic agent for epilepsy.[107] By combining[106,107] μFIPs with recording electrodes, the authors were able to detect seizure-like events (SLEs) in mice induced by local injection of 4-aminopyridine (4AP), then immediately trigger the local delivery of GABA, after which no additional SLEs were observed (Figure 7E). The authors also demonstrated that GABA delivered prior to 4AP injection could prevent SLEs from occurring, suggesting that predictive electrophysiological analysis could potentially be combined with on-demand drug delivery to create closed loop epilepsy treatments (Figure 7E). Notably, because only a small dose of GABA was needed to inhibit neural activity (local concentration of 10^{-5} M), each dose represented less than 1% of the device's total drug loading capacity, indicating the potential for long-term delivery even without replenishment of the reservoir.

As conjugated polymers continue to be explored for drug delivery, it will be important to carefully assess not just the biocompatibility of these materials, but also of the byproducts and contaminants encountered during their syntheses. Additionally, the different on-demand drug delivery architectures should be weighed based on application- and drug-specific requirements regarding drug load, implantation timeframe, and the importance of spatial and temporal control. It will also be important to consider what may happen in the case of premature device failure. For instance, while reservoir-based delivery strategies like the μFIP increase drug loading, they also pose new clinical challenges in the case of reservoir failure, which could expose surrounding tissues to a potentially toxic concentration of the drug.[99] In light of the regulatory barriers associated with conjugated polymers, sufficiently addressing potential safety concerns is particularly crucial for successful clinical translation.

7. Distributed Interface for Electrogenic Tissue

7.1. Spatially Distributed Implantable System

Most electronic medicine relies on integrated and centralized biosignal acquisition and power supply. Implanted power supplies such as batteries often contribute most of the volume in implantable bioelectronic systems and thus prevent their miniaturization and interrogation precision. Furthermore, the physical electronic interconnect for biosignal transmission occupies substantial space, often more than the implantable electrodes or sensors themselves. A wireless system without a physical

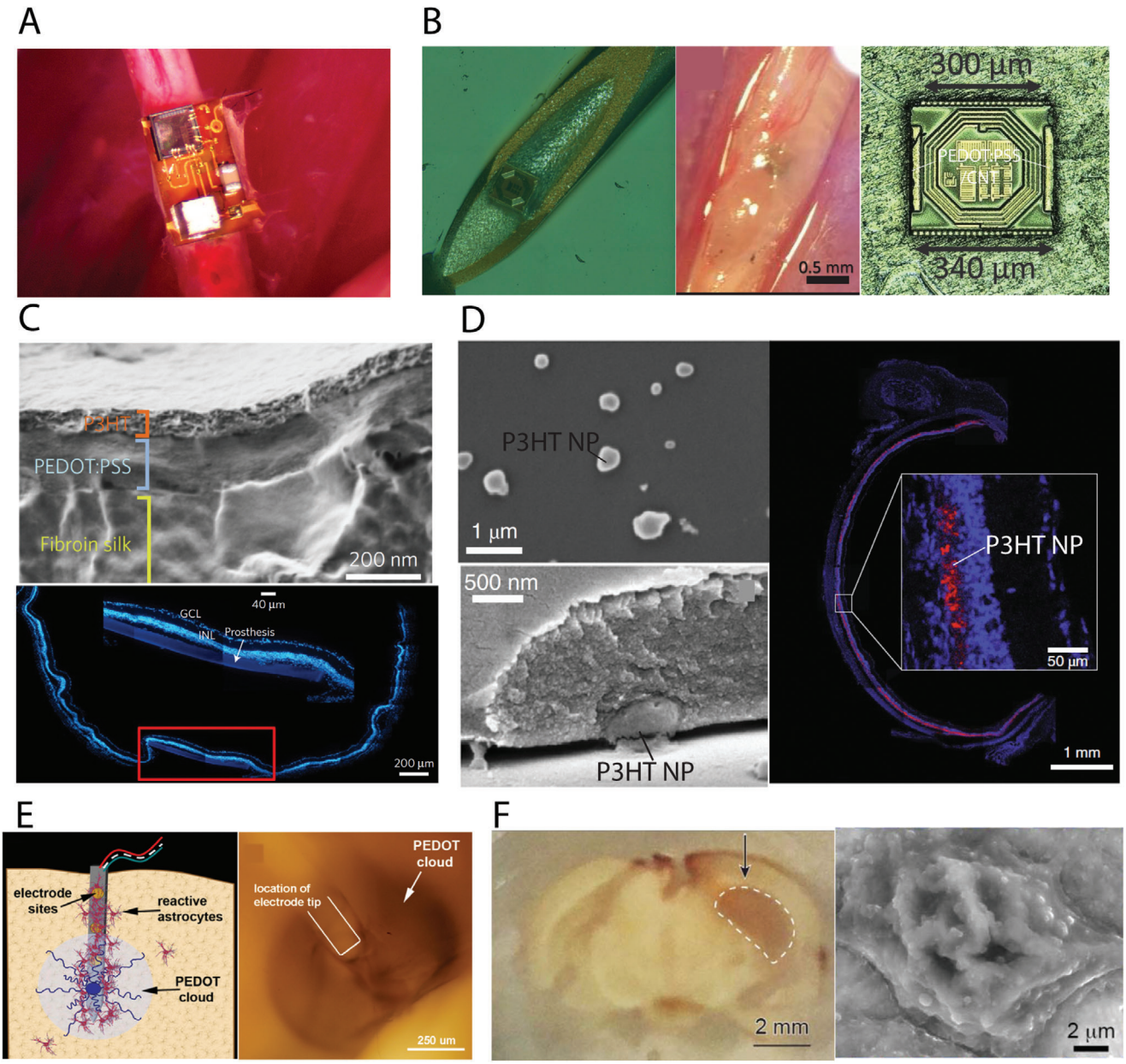

Figure 8. Conjugate polymer as distributed biointerface. A) Wireless ultrasonic peripheral nerve stimulator. Reproduced with permission.[110] Copyright 2018, IEEE. B) Electromagnetically powered 0.009 mm^3 implantable wireless neural stimulator that can be delivered using surgical needles. Reproduced with permission.[111] Copyright 2019, IEEE. C) Photovoltaic prostheses based on P3HT and PEDOT. The subretinal implants led to recovery of light sensitivity and visual acuity that persisted up to 6–10 months after surgery. Reproduced with permission.[117] Copyright 2017, Nature Publishing Group. D) Conjugated polymer nanoparticles (P3HT NPs) mediate light-evoked stimulation of retinal neurons and persistently rescue visual functions when subretinally injected in a rat model of retinitis pigmentosa. Reproduced with permission.[118] Copyright 2020, Nature Publishing Group. E) Polymerizing PEDOT directly into brain tissue from a neural electrode bypassed the surrounding glial scar to reduce the electrochemical impedance. Reproduced with permission.[121] Copyright 2007, Institute of Physics Publishing. F) Genetically instructing specific living neurons to guide chemical synthesis of PNAI at the cell membrane. Reproduced with permission.[124] Copyright 2020, AAAS.

(or materialized) interconnect between the biointerface and signal processing unit could potentially reduce invasiveness and allow higher bandwidths. Ultrasound can power a wireless neural interface for electrophysiological stimulation.[108,109] Johnson et al. developed StimDust, a peripheral nerve stimulator that received ultrasound input and converted it into electrical stimulation with a piezocrystal[110] (**Figure 8**A). Individual Stimdust with a volume of 6.5 mm^3 has been demonstrated to activate the sciatic nerve of anesthetized rodents. PEDOT:PSS was electroplated on Au electrode to further reduce the electrochemical impedance.

Electromagnetic energy coupling is another option for wireless communication. Khalifa et al. reported an electromagnetically powered 2-coil wireless system, the smallest implantable free-floating neural stimulator with a device (including integrated

circuit, electrodes and coil) volume of only 0.009 mm^3. The device was small enough to be delivered by a surgical needle as an injectable neurostimulator (Figure 8B). Inkjet-printed PEDOT:PSS/CNT electrodes at the cross-sectional area of the silicon dies substantially reduced impedance and allowed effective neuromodulation in vivo.[111]

Near-infrared (NIR) radiation at 760 – 1500 nm wavelength can also be used to deliver energy to implantable electronics thanks to its high penetration depth (4 – 10 cm).[112] Pyroelectric materials like polyvinylidene difluoride (PVDF) can be sandwiched between two PEDOT:PSS electrodes to construct a pyroelectric generator to power the neural interface. Upon NIR irradiation, the device was able to electrically stimulate the gastrocnemius muscle of a frog. The high NIR transmittance of PEDOT:PSS prevented high local temperature accumulation and allowed stacking of multiple PEDOT:PSS/PVDF/PEDOT:PSS structures to increase output voltage.[113]

As a p-type conjugated polymer with good biocompatibility, poly(3-hexylthiophene) (P3HT) can convert visible light into electrical stimulation for retinal prosthesis.[114] Excitons generated from P3HT upon illumination can be collected by an organic anode, PEDOT:PSS. Poly(3-hexylthiophene)/[6,6]-phenyl-C61-butyric acid methyl ester (P3HT/PCBM) blend can function as an organic photovoltaic retinal interface. Ghezzi et al. demonstrated restoration of light sensitivity in explants of blind rat retinas without PCBM by using just P3HT and PEDOT:PSS, relying on the capacitive charging of the polymer–electrolyte interface rather than charge transfer in conventional solar cells.[115] Excellent flexibility of the PEDOT:PSS and P3HT enabled a foldable thin-film device structure that could be delivered via a small scleral incision and conform to the curved eye surface.[116,117] The organic photovoltaic prosthesis was capable of wide-angle (visual angle of 46.3 degrees) and high-density (2215 stimulating pixels) stimulation on retinal ganglion cell. Maya-Vetencourt et al. demonstrated that the organic photovoltaic film after implantation rescues light sensitivity and spatial acuity in retinitis pigmentosa for 6–10 months in vivo[117](Figure 8C). This work showed the possibility of long-term neuronal photostimulation with biocompatible conjugated polymer devices. The pixel density of the flexible film-based retinal prosthesis was still an order of magnitude lower than the mosaic of foveal cones (4-5 μm) in healthy eyes, and therefore yields a poor spatial resolution. The same research group recently reported a P3HT nanoparticle (≈300 nm in size) system that can be directly injected into subretinal space[118](Figure 8D). The nanoparticle was tightly wrapped by cell membrane extracellularly, forming a 20 nm cleft and therefore a high junction resistance for effective localized stimulation. The photocurrent of capacitive origin triggered millivolt-level depolarization on multiple sites on the cell membrane and elicited action potential when membrane potential from temporospatial summation of cell-P3HT nanoparticle induced potential surpassed the threshold. The liquid retinal prosthesis, as a non-genetic photostimulator, allows a minimally invasive injection procedure and rescued sensitivity in a blind rodent model with high spatial resolution and very prolonged effects. Although not demonstrated in human clinical studies yet, distributed conjugated polymer-based devices have the potential for treating patients with degenerative blindness without the need for the bulky power supply and cameras used in conventional electrical stimulation systems.

7.2. In Vivo Synthesized Bottom-Up Neural Interface

Implanting prefabricated electronics into biological tissue for a long time has been regarded as the default neural interface configuration. In situ formation of neural interface, referred to here as bottom-up neural interfacing, offers a different but exciting path toward seamless biointegration. Conjugated polymers have unique advantages for in situ synthesis or assembly in a bioenvironment at body temperature. One can leverage the polymerization of conjugated polymers at defined spatial locations to construct neural interfaces in a bottom-up fashion. An early attempt polymerized polypyrrole into a porcine pericardium. However, it used cytotoxic chemical-initiated polymerization and failed to achieve electronic functionality.[119] In another study, researchers chemically oxidize biocompatible 3,4-ethylenedioxylthiophene (EDOT) monomers by Fe^{3+} in situ on acellular muscle tissue constructs, rather than living tissue.[120] Richardson-Burns et al. demonstrated the first direct polymerization of PEDOT in living neural tissue[121] (Figure 8E). In the electrochemical polymerization, nanoscale PEDOT filaments grew out from a gold electrode and formed a cloud of conducting polymer deeply integrated with neural tissues. The PEDOT filaments extending into the extracellular matrix substantially lowered the electrochemical impedance for improved electrical communication between neurons and the neurodevice. Beside, this PEDOT cloud with a few hundred microns to millimeter size could penetrate electrically insulating glial scar tissue, which is around 0.1 -0.15 mm in thickness, and thus has the potential to overcome the challenge of device failure due to foreign body responses. In vivo polymerized PEDOT in rat cerebral cortex improved action potential signal quality with lower recording noise and higher signal-to-noise ratio.[122]

Ouyang et al. further studied the long-term biocompatibility of the in vivo polymerized PEDOT as a potential chronic neural implant.[123] In this study, a microcannula delivered EDOT monomer into the dorsal hippocampus for spatially-targeted electrochemical deposition. In vivo polymerization of PEDOT did not impair the rat's ability to perform the hippocampus-dependent behavioral task of delayed alternation (DA). Although polymerized PEDOT can reduce electrochemical impedance by formation of electrical contact across the scar tissue in the brain, secondary immunoresponse characterized by ED1 and GFAP biomarkers was observed after 2 weeks of polymerization. Further optimization of electrochemical polymerization parameters is required to prevent secondary damage (during polymerization) to the interfaced tissue.

Current neuroelectronic interfaces lack genetic specificity and therefore are unable to selectively interface with specific cellular types. Liu et al. developed a genetically targeted chemical assembly method to introduce conducting polymers directly onto cell membranes[124] (Figure 8F). Humanized version of ascorbate peroxidase Apex2 was selectively expressed in a specific neuronal type and was used to catalyze the polymerization of conducting polymer in the presence of a low concentration of hydrogen peroxide. Polyaniline dimer, rather than monomer, was used to reduce the oxidation potential, so that polymerization could occur at physiological conditions. The polyaniline coated onto cell membranes increased membrane capacitance and therefore reduced the action potential amplitude, which could be used to modulate cell membrane properties. As an example, the

authors reduced the pumping frequency of pharyngeal muscle in *Caenorhabditis elegans* by using the inhibitory role of polyaniline coated on the neurons. This new method of conducting polymer assembly has potential for clinical application where genetic specificity is required. Further improvement is needed, including minimizing chronic cytotoxicity in mammals and increasing electrical conductivity of the synthesized polymer, as is addressing regulatory considerations surrounding genetic modification of cells.

8. Conclusion and Outlook

The repertoire of unique properties in conjugated polymers has substantially expanded over the past decades and is continuously growing. Those unique properties address two of the most important challenges in implantable electronic medicine. The two challenges faced by current implantable bioelectronics are (1) electrical: how to efficiently facilitate ionic-mediated charge transport at the tissue-electronic interface, and (2) mechanical: how to maintain seamless electronic contact to living tissue and co-exist with minimal disturbance to normal biological activity. Conjugated polymers, especially conducting polymers with mixed ionic and electronic conductivity, contribute to low electrochemical impedance of electrodes, high transconductance of electrochemical transistors, and high ion mobility of regenerative electrical patches. Meanwhile, tissue-like mechanical properties, including softness, flexibility, and stretchability, allow a stable and adaptive interface to couple with dynamically moving or rapidly growing electrogenic tissue, and lay the foundation for chronic, mechanically transparent, immunoresponse-free, and seamless bioelectronic integration. Additionally, the tunable redox state of conjugated polymers allows for controlled release of pharmaceutical drugs by doping and de-doping. Looking forward, development in this area will continue in the direction of tissue-mimicking, personalized, and precision electronic medicine.

Conjugated polymer-based implantable electronics show promise in treating cardiac disease, neurological disorders, and other chronic disease. Currently, PEDOT-based ECoG electrode arrays for epilepsy have been tested on 30 human subjects and are furthest along the pipeline of clinical translation.[57] However, most other works have demonstrated potential so far only in small animal models (e.g., rodents). To move beyond small animal models to big animal models, clinical studies, and eventually clinical adoption, certain significant challenges will still need to be overcome. Compared with existing inorganic bioelectronic interfaces, aqueous stability of conducting polymers remains one of the biggest challenges to extend their lifetime. Some implantable electronics such as Intracranial electroencephalography (iEEG) last a few weeks inside the human body. Others such as vagus nerve stimulators expect to last more than 5 years. Yet, stability experiments (e.g., accelerated aging test) on conjugated polymers at such time scales are rare. To overcome stability limitations, chemical strategies can be devised such as direct crosslinking, double network formation, or self-doping to minimize disintegration of the dopant. Through molecular engineering directly on the backbone and/or side chain of the conjugated polymers, we can further improve their electrical conductivity and even introduce new functionality such as in vivo biodegradability that can prevent additional surgeries for removing the implant after treatment is completed.

Reliable sterilization techniques for operative procedures are also required. It has been established that autoclave,[56] ethylene oxide[117] and gamma-ray radiation[125] do not significantly change the electronic performance of PEDOT:PSS and PPy, respectively, but suitable sterilization methods for other conjugated polymers are still lacking. Reliable and scalable microfabrication methods to pattern soft conjugated polymers also need to be developed. Photolithography-compatible fabrication schemes are especially important to construct fully encapsulated, multilayered device structures and high spatial resolution devices for precise communication at the bioelectronic interface. Lastly, acquiring FDA approval for commercialization requires extensive evaluation of clinical safety and efficacy. Especially for novel materials such as conjugated polymers stringent biocompatibility, in-body stability, and cytotoxicity testing are required to minimize their risk to the patients.

Acknowledgements

Z.B. acknowledges support from the National Science Foundation Future Manufacturing Program (award no. 2037164). Y.L. thanks the financial support from Agency for Science, Technology and Research (A*STAR) under its AME Programmatic Funding Scheme (Project #A18A1b0045).

Conflict of Interest

The authors declare no conflict of interest.

Keywords

bioelectronics, clinical translation, conjugated polymers, implantable electronics

Received: November 2, 2020
Revised: December 13, 2020
Published online: April 25, 2021

[1] Allied Market Research. Medical Implants Market – Growth, Global Share, Industry Overview, Analysis, Trends Opportunities and Forecast 2014–2020, https://www.alliedmarketresearch.com/medical-implants-market (accessed: November 2020).
[2] N. K. Guimard, N. Gomez, C. E. Schmidt, *Prog. Polym. Sci.* **2007**, *32*, 876.
[3] C. Zhu, L. Liu, Q. Yang, F. Lv, S. Wang, *Chem. Rev.* **2012**, *112*, 4687.
[4] U. Lange, N. V. Roznyatovskaya, V. M. Mirsky, *Anal. Chim. Acta* **2008**, *614*, 1.
[5] J. Pecher, S. Mecking, *Chem. Rev.* **2010**, *110*, 6260.
[6] X. Guo, M. Baumgarten, K. Müllen, *Prog. Polym. Sci.* **2013**, *38*, 1832.
[7] C. Li, H. Bai, G. Shi, *Chem. Soc. Rev.* **2009**, *38*, 2397.
[8] A. Malinauskas, *Polymer* **2001**, *42*, 3957.
[9] T. Nezakati, A. Seifalian, A. Tan, A. M. Seifalian, *Chem. Rev.* **2018**, *118*, 6766.
[10] V. D. Mihailetchi, H. Xie, B. De Boer, L. J. A. Koster, P. W. M Blom, *Adv. Funct. Mater.* **2006**, *16*, 699.
[11] G. Heywang, F. Jonas, *Adv. Mater.* **1992**, *4*, 116.
[12] H. Letheby, *J. Chem. Soc.* **1862**, *15*, 161.

[13] R. McNeill, R. Siudak, J. H. Wardlaw, D. E. Weiss, *Aust. J. Chem.* **1963**, *16*, 1056.
[14] W. Zeng, et al., *Adv. Mater.* **2014**, *26*, 5310.
[15] T. R. Ray, et al., *Chem. Rev.* **2019**, *119*, 5461.
[16] H. Teymourian, et al., *ACS Sens.* **2020**, *5*, 2679.
[17] M. Jaiswal, R. Menon, *Polym. Int.* **2006**, *55*, 1371.
[18] E. Stavrinidou, et al., *Adv. Mater.* **2013**, *25*, 4488.
[19] C. Deslouis, T. El Moustafid, M. M. Musiani, B. Tribollet, *Electrochim. Acta* **1996**, *41*, 1343.
[20] H. Yuk, B. Lu, X. Zhao, *Chem. Soc. Rev.* **2019**, *48*, 1642.
[21] J. Rivnay, S. Inal, B. A. Collins, M. Sessolo, E. Stavrinidou, X. Strakosas, C. Tassone, D. M. Delongchamp, G. G. Malliaras, *Nat. Commun.* **2016**, *7*.
[22] S. Wang, M. W. Urban, *Nat. Rev. Mater.* **2020**, *5*, 562.
[23] H. Tran, V. R. Feig, K. Liu, Y. Zheng, Z. Bao, *Macromolecules* **2019**, *52*, 3965.
[24] J. Y. Oh, et al., *Nature* **2016**, *539*, 411.
[25] H. Tran, V. R. Feig, K. Liu, Z. Bao, *Proc. Volume 11464, Physical Chemistry of Semiconductor Materials and Interfaces XIX*, SPIE, Bellingham, WA **2020**.
[26] K. Kenry, B. Liu, *Biomacromolecules* **2018**, *19*, 1783.
[27] Y. Lu, A. A. Aimetti, R. Langer, Z. Gu, *Nat. Rev. Mater.* **2016**, *2*, 16075.
[28] J. Y. Lee, C. E. Schmidt, *J. Biomed. Mater. Res., Part A* **2015**, *103*, 2126.
[29] G. Oyman, et al., *RSC Adv.* **2014**, *4*, 53411.
[30] A. Gelmi, M. J. Higgins, G. G. Wallace, *Biomaterials* **2010**, *31*, 1974.
[31] H. Zhang, P. J. Molino, G. G. Wallace, M. Higgins, *Sci. Rep.* **2015**, *5*, 13334.
[32] C. Boehler, et al., *Biomaterials* **2017**, *129*, 176.
[33] D. Svirskis, J. Travas-Sejdic, A. Rodgers, S. Garg, *J. Controlled Release* **2010**, *146*, 6.
[34] Y. Liu, et al., *Nat. Biomed. Eng.* **2019**, *3*, 58.
[35] V. R. Feig, H. Tran, M. Lee, Z. Bao, *Nat. Commun.* **2018**, *9*, 2740.
[36] P. Moshayedi, et al., *Biomaterials* **2014**, *35*, 3919.
[37] J. W. Salatino, K. A. Ludwig, T. D. Y. Kozai, E. K Purcell, *Nat. Biomed. Eng.* **2017**, *1*, 862.
[38] M. Huse, *Nat. Rev. Immunol.* **2017**, *17*, 679.
[39] L. R. Hochberg, et al., *Nature* **2006**, *442*, 164.
[40] R. Mukamel, I. Fried, *Annu. Rev. Psychol.* **2012**, *63*, 511.
[41] S. N. Flesher, et al., *Sci. Transl. Med.* **2016**, *8*, 361ra141.
[42] G. K. Anumanchipalli, J. Chartier, E. F. Chang, *Nature* **2019**, *568*, 493.
[43] P. Kwan, S. C. Schachter, M. J. Brodie, *N. Engl. J. Med.* **2011**, *365*, 2239.
[44] J. Parvizi, S. Kastner, *Nat. Neurosci.* **2018**, *21*, 474.
[45] T. Matsuo, et al., *Front. Syst. Neurosci.* **2011**, *5*, 34.
[46] A. Schander, et al., *IEEE Sens. J.* **2019**, *19*, 820.
[47] E. Castagnola, et al., *IEEE Trans. Neural Syst. Rehabil. Eng.* **2015**, *23*, 342.
[48] D. H. Kim, et al., *Nat. Mater.* **2010**, *9*, 511.
[49] W. Lee, et al., *Sci. Adv.* **2018**, *4*, eaau2426.
[50] A. Blau, et al., *Biomaterials* **2011**, *32*, 1778.
[51] K. Noe, et al., *JAMA Neurol.* **2013**, *70*, 1003.
[52] E. F. Chang, *Neuron* **2015**, *86*, 68.
[53] M. R. Abidian, D. C. Martin, *Adv. Funct. Mater.* **2009**, *19*, 573.
[54] D. Khodagholy, et al., *Nat. Neurosci.* **2015**, *18*, 310.
[55] D. Khodagholy, et al., *Adv. Mater.* **2011**, *23*, H268.
[56] M. Ganji, et al., *Adv. Funct. Mater.* **2018**, *28*, 1700232.
[57] A. C. Paulk, et al., *Cerebral Cortex* **2021**, https://doi.org/10.1093/cercor/bhab040.
[58] R. M. Owens, G. G. Malliaras, *MRS Bull.* **2010**, *35*, 449.
[59] B. D. Paulsen, K. Tybrandt, E. Stavrinidou, J. Rivnay, *Nat. Mater.* **2020**, *19*, 13.
[60] D. Khodagholy, et al., *Nat. Commun.* **2013**, *4*, 1575.
[61] D. Khodagholy, et al., *Nat. Commun.* **2013**, *4*, 2133.
[62] G. C. Faria, D. T. Duong, A. Salleo, *Org. Electron.* **2017**, *45*, 215.
[63] C. Cea, et al., *Nat. Mater.* **2020**, *19*, 679.
[64] W. Lee, et al., *Proc. Natl. Acad. Sci. USA* **2017**, *114*, 10554.
[65] J. P. Seymour, N. B. Langhals, D. J. Anderson, D. R. Kipke, *Biomed. Microdevices* **2011**, *13*, 441.
[66] J. E. Chung, et al., *Neuron* **2019**, *101*, 21.
[67] C. Bodart, et al., *ACS Appl. Mater. Interfaces* **2019**, *11*, 17226.
[68] B. Wei, J. Liu, L. Ouyang, C. C. Kuo, D. C. Martin, *ACS Appl. Mater. Interfaces* **2015**, *7*, 15388.
[69] J. A. Perge, et al., *J. Neural Eng.* **2013**, *10*, 036004.
[70] D. H. Szarowski, et al., *Brain Res.* **2003**, *983*, 23.
[71] E. Musk, *J. Med. Internet Res.* **2019**, *21*, 16194.
[72] D. H. Kim, J. A. Wiler, D. J. Anderson, D. R. Kipke, D. C. Martin, *Acta Biomater.* **2010**, *6*, 57.
[73] X. S. Zheng, et al., *Acta Biomater.* **2020**, *103*, 81.
[74] C. Hassler, T. Boretius, T. Stieglitz, *J. Polym. Sci., Part B: Polym. Phys.* **2011**, *49*, 18.
[75] C. Russell, A. D. Roche, S. Chakrabarty, *Int. J. Intell. Robot. Appl.* **2019**, *3*, 11.
[76] D. Qi, et al., *Adv. Mater.* **2017**, *29*, 1702800.
[77] M. Ganji, A. Tanaka, V. Gilja, E. Halgren, S. A. Dayeh, *Adv. Funct. Mater.* **2017**, *27*, 1703018.
[78] V. A. Pavlov, K. J. Tracey, *Nat. Rev. Endocrinol.* **2012**, *8*, 743.
[79] S. Breit, A. Kupferberg, G. Rogler, G. Hasler, *Front. Psychiatry* **2018**, *9*, 44.
[80] J. Y. Lee, C. A. Bashur, A. S. Goldstein, C. E. Schmidt, *Biomaterials* **2009**, *30*, 4325.
[81] S. Song, et al., *Sci. Rep.* **2019**, *9*, 19565.
[82] J. Song, et al., *Front. Mol. Neurosci.* **2016**, *9*.
[83] G. Shi, M. Rouabhia, Z. Wang, L. H. Dao, Z. Zhang, *Biomaterials* **2004**, *25*, 2477.
[84] T. Lei, et al., *Proc. Natl. Acad. Sci. USA* **2017**, *114*, 5107.
[85] D. Mawad, et al., *J. Mater. Chem.* **2011**, *21*, 5555.
[86] C. Ning, Z. Zhou, G. Tan, Y. Zhu, C. Mao, *Prog. Polym. Sci.* **2018**, *81*, 144.
[87] A. J. Petty, R. L. Keate, B. Jiang, G. A. Ameer, J. Rivnay, *Chem. Mater.* **2020**, *32*, 4095.
[88] J. H. Samuels-Reid, J. U. Cope, *JAMA Pediatr.* **2016**, *170*, 1035.
[89] A. F. Samdani, et al., *Eur. Spine J.* **2015**, *24*, 1533.
[90] Y. Liu, et al., *Nat. Biotechnol.* **2020**, *38*, 1031.
[91] S. M. Narayan, K. Shivkumar, D. E. Krummen, J. M. Miller, W. J. Rappel, *Circ.: Arrhythmia Electrophysiol.* **2013**, *6*, 58.
[92] L. Xu, et al., *Nat. Commun.* **2014**, *5*.
[93] J. Liu, et al., *Proc. Natl. Acad. Sci. USA* **2020**, *117*, 14769.
[94] A. Burnstine-Townley, Y. Eshel, N. Amdursky, *Adv. Funct. Mater.* **2020**, *30*, 1901369.
[95] S. Chen, et al., *J. Controlled Release* **2020**, *320*, 73.
[96] D. Mawad, et al., *Sci. Adv.* **2016**, *2*, 1601007.
[97] L. Wang, et al., *Adv. Funct. Mater.* **2016**, *26*, 4293.
[98] S. Liang, et al., *Adv. Mater.* **2018**, *30*, 1704235.
[99] C. A. R. Chapman, E. A. Cuttaz, J. A. Goding, R. A Green, *Appl. Phys. Lett.* **2020**, *116*, 010501.
[100] J. Ge, E. Neofytou, T. J. Cahill, R. E. Beygui, R. N. Zare, *ACS Nano* **2012**, *6*, 227.
[101] N. Hosseini-Nassab, D. Samanta, Y. Abdolazimi, J. P. Annes, R. N. Zare, *Nanoscale* **2017**, *9*, 143.
[102] D. Samanta, N. Hosseini-Nassab, A. D. McCarty, R. N. Zare, *Nanoscale* **2018**, *10*, 9773.
[103] A. Puiggalí-Jou, L. J. Del Valle, C. Alemán, *ACS Biomater. Sci. Eng.* **2020**, *6*, 2135.
[104] D. T. Simon, et al., *Nat. Mater.* **2009**, *8*, 742.
[105] A. Jonsson, et al., *Sci. Adv.* **2015**, *1*, e1500039.
[106] I. Uguz, et al., *Adv. Mater.* **2017**, *29*, 1701217.
[107] C. M. Proctor, et al., *Sci. Adv.* **2018**, *4*, eaau1291.

[108] D. Seo, et al., *Neuron* **2016**, *91*, 529.
[109] D. Seo, J. M. Carmena, J. M. Rabaey, E. Alon, M. M. Maharbiz, arXiv:1307.2196 **2013**
[110] B. C. Johnson, et al., in *2018 IEEE Custom Integrated Circuits Conf. (CICC)*, IEEE, Piscataway, NJ **2018**.
[111] A. Khalifa, et al., *IEEE Trans. Biomed. Circuits Syst.* **2019**, *13*, 971.
[112] R. Weissleder, *Nat. Biotechnol.* **2001**, *19*, 316.
[113] W. Jiang, et al., *RSC Adv.* **2018**, *8*, 15134.
[114] M. R. Antognazza, et al., *Adv. Healthcare Mater.* **2016**, *5*, 2271.
[115] D. Ghezzi, et al., *Nat. Photonics* **2013**, *7*, 400.
[116] L. Ferlauto, et al., *Nat. Commun.* **2018**, *9*, 992.
[117] J. F. Maya-Vetencourt, et al., *Nat. Mater.* **2017**, *16*, 681.
[118] J. F. Maya-Vetencourt, et al., *Nat. Nanotechnol.* **2020**, *15*, 698.
[119] E. Khor, H. C. Li, A. Wee, *Biomaterials* **1995**, *16*, 657.
[120] A. Peramo, et al., *Tissue Eng., Part A* **2008**, *14*, 423.
[121] S. M. Richardson-Burns, J. L. Hendricks, D. C. Martin, *J. Neural Eng.* **2007**, *4*, L6.
[122] S. J. Wilks, A. J. Woolley, L. Ouyang, D. C. Martin, K. J. Otto, *Proc. of the Annual Int. Conf. of the IEEE Engineering in Medicine and Biology Society*, IEEE, Piscataway, NJ **2011**.
[123] L. Ouyang, C. L. Shaw, C. C. Kuo, A. L. Griffin, D. C. Martin, *J. Neural Eng.* **2014**, *11*, 026005.
[124] J. Liu, et al., *Science* **2020**, *367*, 1372.
[125] S. Kim, et al., *Sci. Rep.* **2018**, *8*, 3721.

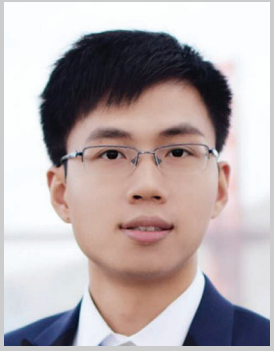

Yuxin Liu is a research scientist in Institute of Materials Research and Engineering (IMRE), A*STAR. He received Ph.D. degree in bioengineering from Stanford University in 2019. During his Ph.D. training in Professor Zhenan Bao's group, he conducted research on soft electronics, wearable device, and morphing neural interface. His research interest includes tissue-mimicking brain-machine interface and translation research on precision electronic medicine.

Vivian Rachel Feig is a postdoctoral research fellow at the Brigham and Women's Hospital, Harvard Medical School, under the supervision of Prof. Robert Langer and Prof. Giovanni Traverso. She received her Ph.D. in materials science and engineering in 2020 from Stanford University with Prof. Zhenan Bao. As a National Defense Science and Engineering Graduate (NDSEG) Research Fellow at Stanford, she developed soft conductive materials for stable long-term bioelectronic interfaces.

Zhenan Bao is a K.K. Lee Professor of Chemical Engineering at Stanford University. Prior to joining Stanford in 2004, she was a Distinguished Member of Technical Staff in Bell Labs, Lucent Technologies from 1995-2004. She received her Ph.D. in chemistry from the University of Chicago in 1995. She pioneered a number of design concepts for organic electronic materials. Her work has enabled flexible electronic circuits and displays. In her recent work, she has developed skin-inspired organic electronic materials, which resulted in unprecedented performance or functions in medical devices, energy storage and environmental applications. Bao is a member of the National Academy of Engineering and the National Academy of Inventors.